Magnetization of underdoped YBa2Cu3Oy above the irreversibility field

Yu, Jing Fei; Ramshaw, B. J.; Kokanović, Ivan; Modic, K. A.; Harrison, N.; Day, James; Liang, Ruixing; Hardy, W. N.; Bonn, D. A.; McCollam, A.; ...

Source / Izvornik: **Physical review B: Condensed matter and materials physics, 2015, 92**

Journal article, Published version
Rad u časopisu, Objavljena verzija rada (izdavačev PDF)

https://doi.org/10.1103/PhysRevB.92.180509

Permanent link / Trajna poveznica: https://urn.nsk.hr/urn:nbn:hr:217:010213

Rights / Prava: In copyright / Zaštićeno autorskim pravom.

Download date / Datum preuzimanja: **2024-07-16**

Repository / Repozitorij:

Repository of the Faculty of Science - University of Zagreb

DIGITALNI AKADEMSKI ARHIVI I REPOZITORIJI

PHYSICAL REVIEW B **92**, 180509(R) (2015)

Magnetization of underdoped $YBa_2Cu_3O_y$ above the irreversibility field

Jing Fei Yu,[1,*] B. J. Ramshaw,[2] I. Kokanović,[3,4] K. A. Modic,[2] N. Harrison,[2] James Day,[5] Ruixing Liang,[5,6] W. N. Hardy,[5,6] D. A. Bonn,[5,6] A. McCollam,[7] S. R. Julian,[1,6] and J. R. Cooper[3]

[1]*Department of Physics, University of Toronto, Toronto, Ontario M5S 1A7, Canada*
[2]*Los Alamos National Laboratory, Mail Stop E536, Los Alamos, New Mexico 87545, USA*
[3]*Cavendish Laboratory, University of Cambridge, Cambridge CB3 0HE, United Kingdom*
[4]*Department of Physics, Faculty of Science, University of Zagreb, P.O. Box 331, Zagreb, Croatia*
[5]*Department of Physics and Astronomy, University of British Columbia, Vancouver, British Columbia V6T 1Z1, Canada*
[6]*Canadian Institute for Advanced Research, 180 Dundas St. W, Toronto, Ontario M5S 1Z8, Canada*
[7]*High Field Magnet Laboratory (HFML-EMFL), Radboud University, 6525 ED Nijmegen, The Netherlands*

(Received 18 September 2015; revised manuscript received 1 November 2015; published 23 November 2015)

Torque magnetization measurements on $YBa_2Cu_3O_y$ (YBCO) at doping $y = 6.67$ ($p = 0.12$), in dc fields (B) up to 33 T and temperatures down to 4.5 K, show that weak diamagnetism persists above the extrapolated irreversibility field $H_{\mathrm{irr}}(T = 0) \approx 24$ T. The differential susceptibility dM/dB, however, is more rapidly suppressed for $B \gtrsim 16$ T than expected from the properties of the low field superconducting state, and saturates at a low value for fields $B \gtrsim 24$ T. In addition, torque measurements on a $p = 0.11$ YBCO crystal in pulsed field up to 65 T and temperatures down to 8 K show similar behavior, with no additional features at higher fields. We offer two candidate scenarios to explain these observations: (a) superconductivity survives but is heavily suppressed at high field by competition with charge-density-wave (CDW) order; (b) static superconductivity disappears near 24 T and is followed by a region of fluctuating superconductivity, which causes dM/dB to saturate at high field. The diamagnetic signal observed above 50 T for the $p = 0.11$ crystal at 40 K and below may be caused by changes in the normal state susceptibility rather than bulk or fluctuating superconductivity. There will be orbital (Landau) diamagnetism from electron pockets and possibly a reduction in spin susceptibility caused by the stronger three-dimensional ordered CDW.

DOI: 10.1103/PhysRevB.92.180509 PACS number(s): 74.72.Gh, 74.25.Bt, 74.25.Ha, 74.25.Op

The possible existence of bulk superconductivity as $T \to 0$ K above the irreversibility field (H_{irr}) [1] in the cuprates has been a long-standing question. Not only is this problem important for our understanding of the cuprates, but also because there is still debate [2,3] about whether Cooper pairs persist in the region of the field-temperature plane where quantum oscillations are seen [4].

Many experimental efforts have been made to address this issue [5–8]. Diamagnetism has consistently been reported using torque magnetometry at high fields in many families of cuprates and it is argued that this observation shows the persistence of Cooper pairs above H_{irr} [5]. For $YBa_2Cu_3O_y$ (YBCO), resistivity measurements have established $H_{\mathrm{irr}}(T = 0)$ to be below 30 T for fields along the c axis for dopings between $p = 0.11$ (OII) and $p = 0.12$ (OVIII) [9]. Moreover, x-ray [10–12], NMR [13], and sound velocity measurements [14] have demonstrated the existence of static charge-density-wave (CDW) order that competes with superconductivity: Reference [12] shows a distinct long-range three-dimensional (3D) order that emerges at high field and continues to grow at 28 T for an OVIII crystal, consistent with that first observed in NMR studies [13]. The CDW is strongest and the suppression of H_{c2} is largest at $p = 0.125$ for YBCO [11,15].

Recent thermal conductivity measurements by Grissonnanche *et al.* [7] show a sharp transition precisely at the extrapolated $H_{\mathrm{irr}}(T = 0) \simeq 22$ T for OII YBCO. They have interpreted this feature (henceforth referred to as H_K) as a signature of H_{c2}, arguing that the end of the rapid rise in thermal conductivity at 22 T reflects a corresponding increase in the mean free path as a result of the sudden disappearance of vortices at H_{c2}. On a crystal with same doping, Marcenat *et al.* [16] show that the specific heat saturates at a field H_{cp}. $H_{cp}(T)$ lies above $H_{\mathrm{irr}}(T)$, but they extrapolate to the same value at $T = 0$ K [16]. In contrast, torque measurements by Yu *et al.* [6] on a crystal with the same doping suggested diamagnetism persisting to fields much higher than H_K. The debate is thus still open.

To resolve this problem, we conducted torque magnetometry measurements of magnetization (M) on two $p = 0.12$ (OVIII, $T_c = 65$ K) crystals in dc fields and one $p = 0.11$ (OII, $T_c = 60$ K) crystal in pulsed fields. The crystals were mounted on piezoresistive cantilevers and placed on a rotating platform, with the CuO_2 planes parallel to the surface of the lever. dc field sweeps, first from 0 to 10 T and later from 0 to 33 T, were performed with the c axis of the OVIII crystal at a small angle θ from the field. The magnetoresistance of the levers was eliminated by subtracting data from the complementary angle ($-\theta$) (see Supplemental Material for raw data [17]). Similar procedures were used for the OII crystal in pulsed magnetic fields up to 65 T. For strongly anisotropic superconductors, where out-of-plane screening currents can be neglected, the torque τ per unit volume V at an angle θ from field B is given by [18] $\tau/V = \frac{1}{2}\chi_D(T)B^2 \sin 2\theta + M_c B \sin\theta$. Here $\chi_D(T) = \chi_c(T) - \chi_{ab}(T)$ is the anisotropic susceptibility in the normal state and M_c is the magnetization from in-plane screening currents for a field of $B \cos\theta$ along the c axis. This is a good approximation when $M_c \gg \chi_D B$ or when the superconducting gap and M_c are both small.

*jfeiyu@physics.utoronto.ca

 ©2015 American Physical Society

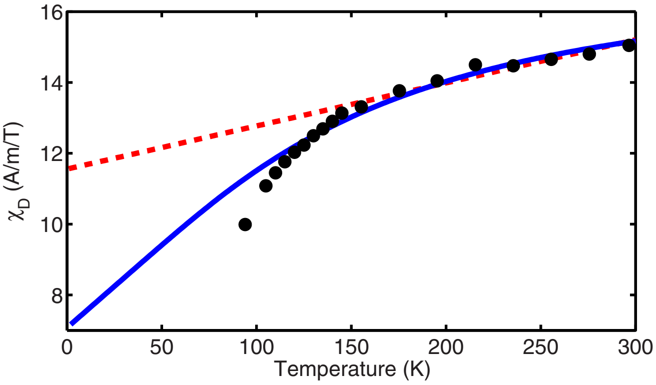

FIG. 1. (Color online) Black dots: high temperature anisotropic susceptibility $\chi_D(T)$ of the OVIII crystal at 10 T. Blue solid line: fit to this data above 120 K using Eq. (1). The parameters $A = 11.09$ A/m/T, $T_F = 680$ K are taken from Ref. [19], while the fit gives $\chi^{VV} = 5.84$ A/m/T, $T^* = 330$ K and $\chi^R(0) = 1.26$ A/m/T; Red dashed line: Linear fit with $\chi(T) = 1.22 \times 10^{-2} \times (T + 948)$, following Ref. [6] but with different parameters. Note that 1×10^{-4} emu/mol = 9.73 A/m/T.

A key challenge with magnetization measurements in the cuprates is the separation of the normal state from the superconducting contributions, because superconducting fluctuations are thought to contribute to $\chi(T)$ even at temperatures far above T_c [18], while $\chi^{\rm normal}$ is temperature dependent to well below T_c. We follow the procedure outlined in Refs. [18,19] and interpret $\chi_D(T)$ in the normal state of underdoped YBCO as arising from the pseudogap and g-factor anisotropy, plus a superconducting fluctuation term that sets in below 120 K. Neglecting isotropic Curie and core susceptibility terms, which do not contribute to τ, the total normal state contribution to $\chi_D(T)$ is [19]

$$\chi_D^{\rm normal}(T) = \chi_D^{PG}(T) + \chi_D^{VV} + \chi_D^R(T), \qquad (1)$$

where χ_D^{VV} is the T-independent Van Vleck susceptibility, $\chi_D^{PG}(T)$ is the pseudogap contribution assuming a V-shaped density of states [20], and $\chi_D^R(T)$ is thought to arise from an electron pocket or Fermi arcs in the region $0.0184 < p < 0.135$. Specifically, $\chi_D^{PG} = A\{1 - y^{-1}\ln[\cosh(y)]\}$, where $A = N_0\mu_B^2$, $y = E_g/2k_BT$, $E_g = k_BT^*$ and T^* is the pseudogap temperature, and $\chi_D^R(T) = \chi^R(0)[1 - \exp(-T_F/T)]$ where T_F is the Fermi temperature. The fit is shown in Fig. 1, along with a linear model for the normal state χ used in Ref. [6]. Both fits agree well with the data for $T \geqslant 120$ K. Our background is almost twice as small as that of the linear fit at $T = 0$ K. Subtraction of the background magnetization using this nonlinear model should thus give a significantly weaker diamagnetic signal at $T \to 0$ K than the linear model would (by about 160 A/m at 30 T).

In Figs. 2(a) and 3(a), we show M_c vs B_z curves at selected temperatures for the OVIII and OII crystals, obtained by subtracting $M_{BG} = \chi_{BG}B_z$, where χ_{BG} is the blue line in Fig. 1, and B_z is the field projected along the crystalline c axis. For the OVIII crystal, at $T = 103$ K, we see that M_c is almost zero. At 58 K, just below T_c, we see significant diamagnetism that gradually tends to about -130 A/m at high field. Figure 2(a) shows that the crystal remains weakly

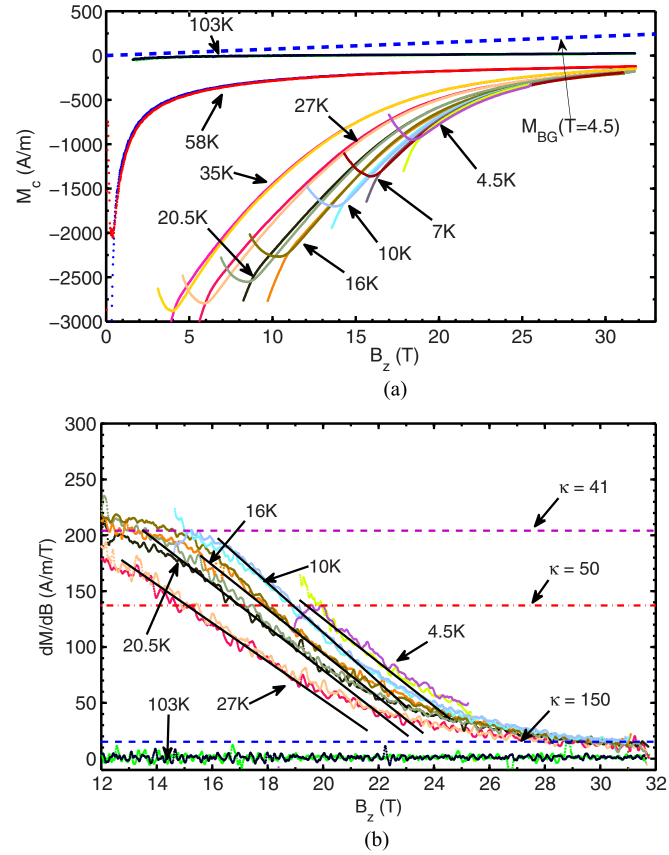

FIG. 2. (Color online) (a) Magnetization (M_c) of the OVIII crystal vs B_z, the field parallel to the c axis. Here $M_c(T,H) = M_{\rm obs}(T,H) - M_{BG}(T,H)$, where $M_{BG} = \chi_D B_z$ and χ_D is the blue line in Fig. 1. Dashed line: M_{BG} at 4.5 K. Diamagnetism is present even at our highest field of 33 T. (b) Differential susceptibility dM/dB of the OVIII crystal vs B_z at selected temperatures. The lines are guides to the eye. We call the characteristic field at which dM/dB departs from linearity H_d. Red: calculated mean field dM/dB near H_{c2} with $\kappa = 50$, with $\kappa = 41$ (purple) and with $\kappa = 150$ (blue).

diamagnetic down to 4.5 K in fields up to 33 T. Similar behavior was found for the OII crystal in pulsed fields. As shown in Fig. 3(a), M_c is still diamagnetic at the highest field $B_z = 63$ T, but has a small value – about -90 A/m at 8 K. Our results differ from those of Yu *et al.* [6]: Our normal state susceptibility is larger than theirs by approximately 8 A/m/T, and after background subtraction, at 10 K and 20 T we find M_c to be up to four times larger (see Supplemental Material for details on the calibration procedure); at 30 T we find about -200 A/m for OII and OVIII rather than their value of -75 A/m. Our estimated uncertainty in $\chi_D(0)$ corresponds to ± 32 A/m in M_c at 33 T and ± 61 A/m at 63 T.

Although the weak diamagnetic signal persists to higher fields, we are able to see a signature in our differential susceptibility dM/dB at fields comparable to H_K (22 T) found by thermal conductivity [7]. In each curve of Figs. 2(b) and 3(b), dM/dB decreases linearly, up to a field we call $H_d(T)$, before saturating to a small but nonzero value. At the lowest temperatures for both OVIII and OII crystals, we find $H_d \approx 24$ T, which is close to the extrapolated $H_{\rm irr}(T = 0)$. This is consistent with the feature at H_K found by thermal

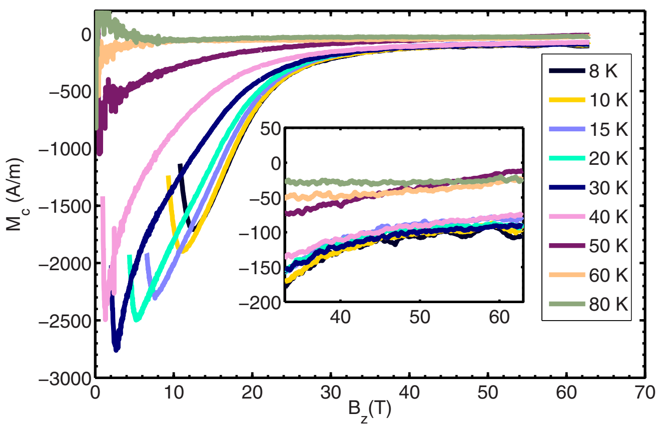

(a)

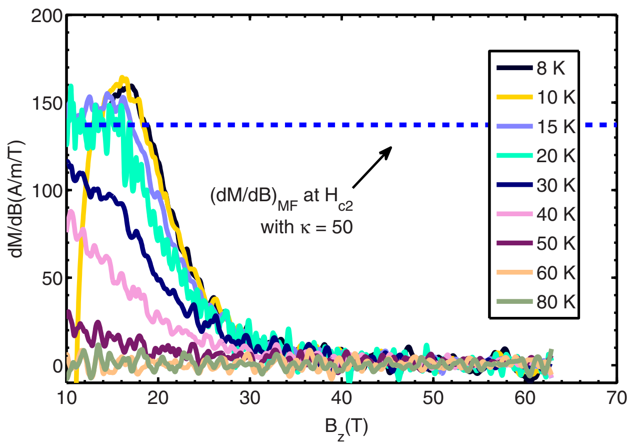

(b)

FIG. 3. (Color online) (a) Magnetization (M_c) of the OII crystal measured in pulsed magnetic field up to $B_z = 63$ T, where $M_c = M_{\rm obs} - M_{BG}$, $M_{BG} = \chi_D B_z$, and χ_D is the blue line in Fig. 1. For clarity only the falling-field sweeps are shown. Diamagnetism is present though extremely weak at high field (inset). The small offset in M_c between the $T \leqslant 40$ K and $T \geqslant 50$ K curves may be due to the transition to long-range CDW order near 40 K in high fields as observed in both sound velocity [14] and NMR [13]. (b) Differential susceptibility for the OII crystal in pulsed field. dM/dB is seen to be small and constant up to the highest field of 63 T. Blue: calculated mean field dM/dB near H_{c2} with $\kappa = 50$.

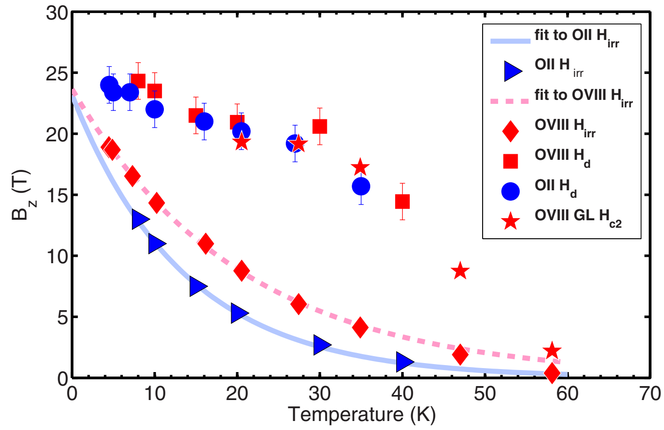

FIG. 4. (Color online) H_d for both OII and OVIII crystals show similar temperature dependencies. Exponential fits to $H_{\rm irr}$ of OII $[23.2\exp(-T/13.5)]$ and OVIII $[23.7\exp(-T/20.5)]$ give extrapolated values $H_{\rm irr}(0) = 23.2$ and 23.7 T. These values are close to the low temperature H_d for both crystals. Note that H_{c2} from GL fits (see main text) connects smoothly to H_d.

conductivity [7], though unlike H_K, H_d does not correspond to a sharp transition. H_d varies very little with temperature for $T < 10$ K, a result that is consistent with the findings of Ref. [7], though the T dependence at high temperatures is not consistent with that found by Refs. [6,16]. Surprisingly, we do not observe in any of our crystals the broad peak in dM/dB reported by Ref. [6].

In highly anisotropic type-II superconductors, the magnetization calculated using mean field (MF) Ginzburg-Landau (GL) theory for an s-wave superconductor, which we use in the absence of a d-wave theory, yields logarithmic behavior at low field (in cgs units), $-4\pi M = \alpha\phi_0/(8\pi\lambda^2)\ln(\beta H_{c2}/H)$ for $0.02 < H/H_{c2} < 0.3$, where α and β are numbers of order 1, ϕ_0 is the flux quantum for Cooper pairs, and λ is the London penetration depth [21]. μSR at low fields has shown a $\sqrt{H}$ field dependence [22] for $\lambda(T = 0)$, but results of tunneling experiments on Bi-2212 imply thermally induced pair breaking near the nodes [23], indicating a weaker field dependence at higher T. Thus, for simplicity, we assume a negligible field dependence of λ. We also assume [21] $\alpha = 0.77$ and $\beta = 1.44$ for $0.02 < H/H_{c2} < 0.3$, in reasonable agreement with later works [24,25], and we fit the low field magnetization and obtain an estimate of $H_{c2}(T)$, shown in Fig. 4. Since our GL values of H_{c2} join smoothly to H_d, it is possible to interpret H_d as the low temperature GL-type H_{c2}.

When $H/H_{c2} > 0.3$, and again using cgs units for an s-wave superconductor, the magnetization is expected to obey $4\pi M = (H - H_{c2})/[(2\kappa^2 - 1)\beta_A]$, where κ is the GL parameter and $\beta_A = 1.16$ is the Abrikosov parameter [26,27]. Figures 2(b) and 3(b) show that for $B > 28$ T, dM/dB has the mean field property of saturating toward a constant value, but this is very small and requires $\kappa \simeq 150$, a value far greater than $\kappa = 50$ given in Ref. [7]. This means that our high field dM/dB is nearly ten times smaller than would be expected. This may be due to the field dependent charge-density-wave (CDW) order within the vortex liquid region [11,12]. The CDW competes with superconductivity and is partially suppressed at low field. As increasing field suppresses superconductivity, the CDW order is gradually restored [14]. The presence of a relatively strong CDW would increase λ and thus increase κ, as illustrated in Fig. 5. A linear region in $M_c(B)$ can also be seen in Fig. 2(a), for $T = 20$ K and $T = 16$ K and $B \leqslant 17$ T, with $\kappa = 41$, and in Fig. 3(a), for $T = 20$ K and $B \leqslant 17$ T, with $\kappa = 50$. These linear regions are not present above 20 K, where $M_c(B)$ is likely to be smeared out by thermal fluctuations. As shown in Fig. 5, for the OVIII crystal, the low field M_c extrapolates to zero around 24 T, consistent with our GL-type H_{c2}. To summarize, clear linear regions, with slopes corresponding to the expected values of κ, have been observed for both doping levels below 20 K.

The value of $H_{c2}(0) \approx H_d \approx 24$ T obtained from these GL analyses may refer to a low field, unreconstructed Fermi

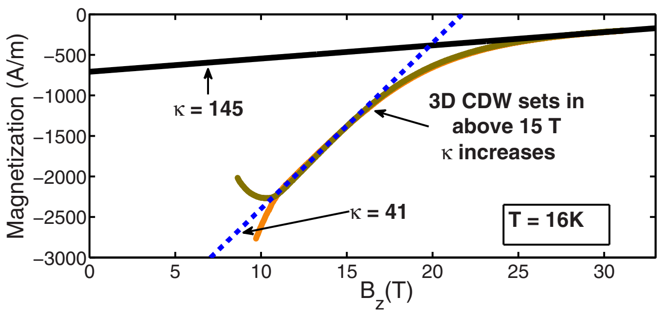

FIG. 5. (Color online) Magnetization data of the OVIII crystal at 16 K. The blue dashed line shows the MF behavior near H_{c2} for an *s*-wave superconductor with $\kappa = 41$. The stronger (3D) CDW sets in above 15 T for OVIII YBCO. At higher fields the data are consistent with $\kappa = 145$ (solid line).

surface. For fields greater than 24 T, we may be observing MF behavior of weak superconductivity arising from the small electron pockets [4,28] resulting from the appearance of CDW order. The GL-type theory we applied assumes *s*-wave superconductivity and we cannot rule out possible *d*-wave effects on the determination of H_{c2}. An obvious possibility is the Volovik effect whereby the Cooper pairs near the nodes on the Fermi surface are broken up, and consequently, λ and κ would increase.

Alternatively, the diamagnetism that we observe above 24 T could be caused by superconducting fluctuations. The OII data in the inset of Fig. 3(a) show that it is ~ -100 A/m between 35 and 63 T. This is five times smaller and falls more quickly with field than predicted by theory [29] for a two-dimensional *s*-wave superconductor at low temperatures and high fields. This is a robust statement because in the clean limit all parameters in the theoretical expression [29] for $M_c(B)$ above H_{c2} are known. Nernst data [30] for OVIII crystal show saturation near 30 T to the negative value expected for an electron pocket. This does not necessarily rule out bulk superconductivity above 30 T because in the presence of a CDW, the vortex core entropy – which dominates the Nernst effect – could be reduced. However, at a qualitative level, the Nernst data between 24 and 30 T may be more consistent with superconducting fluctuations. Since torque magnetization is sensitive to superconducting fluctuations, while thermal conductivity sees only the normal quasiparticles which are the only source of entropy, this may explain why we do not observe the sharp transition at H_K seen in Ref. [7].

Finally, the diamagnetism of -90 A/m observed at 63 T might arise from orbital (Landau) diamagnetism of the electron pockets [31] possibly combined with a suppression of spin susceptibility [32] associated with the stronger (3D) CDW order that sets in above 15 T [12]. The change required would be 1.36 A/m/T in $\chi_D(0)$. This is consistent with the significant decrease in diamagnetism between 40 and 50 K shown in the inset of Fig. 3(a), the region where the 3D CDW seen at high fields goes away [12].

The above discussion highlights the importance of competing CDW and superconductivity instabilities [11,33]. Little is known about the size of the CDW energy gap, or the MF behavior expected for a *d*-wave superconductor just below H_{c2} as $T \to 0$ K. Therefore the linear H dependence of dM/dB we observe below H_d might be a fundamental property of a *d*-wave superconductor. In other words, because of Volovik-type pair breaking effects, the MF transition at H_{c2} could have a discontinuity in d^2M/dB^2, rather than in dM/dB, which is the standard MF result for the second order transition in a conventional *s*-wave superconductor.

In summary, we observe diamagnetism in OVIII YBCO at fields up to 33 T and OII YBCO at fields up to 65 T using torque magnetometry. The analysis uses a different model for the high temperature normal state susceptibility that gives a smaller correction at low temperature compared with earlier models [6]. We also find that dM/dB departs from a linear lower field behavior at fields $H_d \approx H_{\mathrm{irr}}(0) \approx 24$ T, and approaches a constant value at higher fields. We propose two candidate scenarios: a competing order scenario where a fully fledged CDW at high field mostly suppresses the superconductivity so that the diamagnetism at high field could be attributed to bulk superconductivity; or a fluctuation picture in which for $H > H_d$, the system crosses over to superconducting fluctuation behavior. The diamagnetism at 65 T for the OII crystal could arise from the orbital susceptibility of carrier pockets and a reduction in spin susceptibility associated with the stronger 3D CDW order. It would be of interest to develop *d*-wave expressions for the MF magnetization and for the fluctuation contribution in the low temperature, high field regime, for comparison with our data. This could settle the debate over the existence of the high field vortex liquid region.

We thank G. Grissonnanche for useful discussions. This work was generously supported by NSERC under Grant No. RGPGP 170825-13 and No. RGPIN-2014-04554 and CIFAR of Canada, Canada Research Chair, EPSRC (UK) under Grant No. EP/K016709/1, Croatian Science Foundation project (No. 6216), and the Croatian Research Council, MZOS NEWFEL-PRO project No. 19. We thank HFML-RU, a member of the European Magnetic Field Laboratory. The work at LANL was funded by the Department of Energy Basic Energy Sciences program "Science at 100 T." The NHMFL facility is funded by the Department of Energy, the State of Florida, and the National Science Foundation (NSF) Cooperative Agreement No. DMR-1157490.

---

[1] For ease of comparison with Refs. [7] and [6], we use the same units (Tesla) and notation (e.g., H_{irr} and H_{c2}) throughout this Rapid Communication.

[2] S. Banerjee, S. Zhang, and M. Randeria, Nat. Commun. **4**, 1700 (2013).

[3] M. R. Norman and A. H. MacDonald, Phys. Rev. B **54**, 4239 (1996).

[4] N. Doiron-Leyraud, C. Proust, D. LeBoeuf, J. Levallois, J.-B. Bonnemaison, R. Liang, D. A. Bonn, W. N. Hardy, and L. Taillefer, Nature (London) **447**, 565 (2007).

[5] L. Li, Y. Wang, S. Komiya, S. Ono, Y. Ando, G. D. Gu, and N. P. Ong, Phys. Rev. B **81**, 054510 (2010).
[6] F. Yu, M. Hirschberger, T. Loew, G. Li, B. J. Lawson, T. Asaba, J. B. Kemper, T. Liang, J. Porras, G. S. Boebinger, J. Singleton, B. Keimer, L. Li, and N. P. Ong, arXiv:1402.7371.
[7] G. Grissonnanche, O. Cyr-Choinière, F. Laliberté, S. René de Cotret, A. Juneau-Fecteau, S. Dufour-Beauséjour, M.-E. Delage, D. Leboeuf, J. Chang, B. J. Ramshaw, D. A. Bonn, W. N. Hardy, R. Liang, S. Adachi, N. E. Hussey, B. Vignolle, C. Proust, M. Sutherland, S. Krämer, J.-H. Park *et al.*, Nat. Commun. **5**, 3280 (2014).
[8] S. C. Riggs, O. Vafek, J. B. Kemper, J. B. Betts, A. Migliori, F. F. Balakirev, W. N. Hardy, R. Liang, D. A. Bonn, and G. S. Boebinger, Nat. Phys. **7**, 332 (2011).
[9] B. J. Ramshaw, J. Day, B. Vignolle, D. LeBoeuf, P. Dosanjh, C. Proust, L. Taillefer, R. Liang, W. N. Hardy, and D. A. Bonn, Phys. Rev. B **86**, 174501 (2012).
[10] G. Ghiringhelli, M. Le Tacon, M. Minola, S. Blanco-Canosa, C. Mazzoli, N. B. Brookes, G. M. De Luca, A. Frano, D. G. Hawthorn, F. He, T. Loew, M. M. Sala, D. C. Peets, M. Salluzzo, E. Schierle, R. Sutarto, G. A. Sawatzky, E. Weschke, B. Keimer, and L. Braicovich, Science **337**, 821 (2012).
[11] J. Chang, E. Blackburn, A. T. Holmes, N. B. Christensen, J. Larsen, J. Mesot, R. Liang, D. A. Bonn, W. N. Hardy, A. Watenphul, M. V. Zimmermann, E. M. Forgan, and S. M. Hayden, Nat. Phys. **8**, 871 (2012).
[12] S. Gerber, H. Jang, H. Nojiri, S. Matsuzawa, H. Yasumura, D. A. Bonn, R. Liang, W. N. Hardy, Z. Islam, A. Mehta, S. Song, M. Sikorski, D. Stefanescu, Y. Feng, S. A. Kivelson, T. P. Devereaux, Z. X. Shen, C. C. Kao, W. S. Lee, D. Zhu, and J. S. Lee, Science (2015), doi:10.1126/science.aac6257.
[13] T. Wu, H. Mayaffre, S. Krämer, M. Horvatić, C. Berthier, P. L. Kuhns, A. P. Reyes, R. Liang, W. N. Hardy, D. A. Bonn, and M.-H. Julien, Nat. Commun. **4**, 2113 (2013).
[14] D. LeBoeuf, S. Krämer, W. N. Hardy, R. Liang, D. A. Bonn, and C. Proust, Nat. Phys. **9**, 79 (2013).
[15] M. Hücker, N. B. Christensen, A. T. Holmes, E. Blackburn, E. M. Forgan, R. Liang, D. A. Bonn, W. N. Hardy, O. Gutowski, M. V. Zimmermann, S. M. Hayden, and J. Chang, Phys. Rev. B **90**, 054514 (2014).
[16] C. Marcenat, A. Demuer, K. Beauvois, B. Michon, A. Grockowiak, R. Liang, W. Hardy, D. A. Bonn, and T. Klein, Nat. Commun. **6**, 7927 (2015).
[17] See Supplemental Material at http://link.aps.org/supplemental/10.1103/PhysRevB.92.180509 for detailed description of the calibration method used for the cantilever and shows examples of our raw data.
[18] I. Kokanović, D. J. Hills, M. L. Sutherland, R. Liang, and J. R. Cooper, Phys. Rev. B **88**, 060505 (2013).
[19] I. Kokanović, J. R. Cooper, and K. Iida, Europhys. Lett. **98**, 57011 (2012).
[20] J. W. Loram, K. A. Mirza, J. R. Cooper, and J. L. Tallon, J. Phys. Chem. Solids **59**, 2091 (1998).
[21] Z. Hao and J. R. Clem, Phys. Rev. Lett. **67**, 2371 (1991).
[22] J. E. Sonier, S. A. Sabok-Sayr, F. D. Callaghan, C. V. Kaiser, V. Pacradouni, J. H. Brewer, S. L. Stubbs, W. N. Hardy, D. A. Bonn, R. Liang, and W. A. Atkinson, Phys. Rev. B **76**, 134518 (2007).
[23] T. M. Benseman, J. R. Cooper, and G. Balakrishnan, arXiv:1503.00335.
[24] W. V. Pogosov, K. I. Kugel, A. L. Rakhmanov, and E. H. Brandt, Phys. Rev. B **64**, 064517 (2001).
[25] S. Bosma, S. Weyeneth, R. Puzniak, A. Erb, A. Schilling, and H. Keller, Phys. Rev. B **84**, 024514 (2011).
[26] M. Tinkham, *Introduction to Superconductivity*, 2nd ed. (Dover, Mineola, New York, 1996).
[27] Z. Hao and J. R. Clem, Phys. Rev. B **43**, 7622 (1991).
[28] D. LeBoeuf, N. Doiron-Leyraud, J. Levallois, R. Daou, J.-B. Bonnemaison, N. E. Hussey, L. Balicas, B. J. Ramshaw, R. Liang, D. A. Bonn, W. N. Hardy, S. Adachi, C. Proust, and L. Taillefer, Nature (London) **450**, 533 (2007).
[29] V. M. Galitski and A. I. Larkin, Phys. Rev. B **63**, 174506 (2001).
[30] J. Chang, N. Doiron-Leyraud, F. Laliberté, R. Daou, D. LeBoeuf, B. J. Ramshaw, R. Liang, D. A. Bonn, W. N. Hardy, C. Proust, I. Sheikin, K. Behnia, and L. Taillefer, Phys. Rev. B **84**, 014507 (2011).
[31] C. Schlenker, S. S. P. Parkin, and H. Guyot, J. Magn. Magn. Mater. **54-57**, 1313 (1986).
[32] D. C. Johnston, Phys. Rev. Lett. **52**, 2049 (1984).
[33] L. E. Hayward, A. J. Achkar, D. G. Hawthorn, R. G. Melko, and S. Sachdev, Phys. Rev. B **90**, 094515 (2014).